

ACS Spring Meeting 2015, Denver, CO

Stopping Powers from Time-Dependent Density Functional Theory

R.J. Magyar

Sandia National Laboratories

Collaborator: A. Baczewski

Sandia National Laboratories



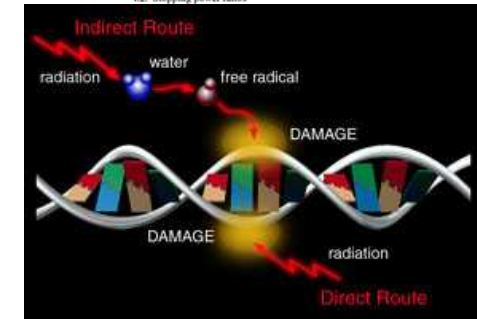
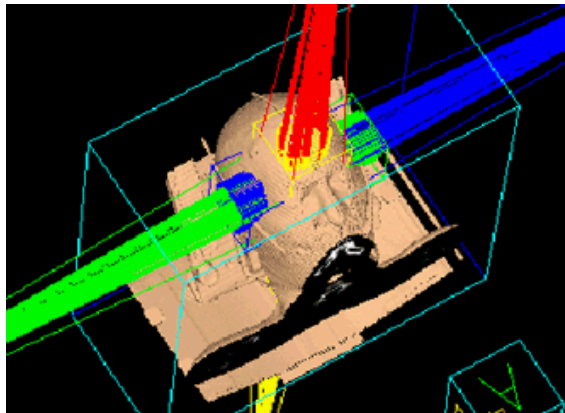
Sandia National Laboratories is a multi program laboratory managed and operated by Sandia Corporation, a wholly owned subsidiary of Lockheed Martin Corporation, for the U.S. Department of Energy's National Nuclear Security Administration under contract DE-AC04-94AL85000.



Importance of Stopping Power



- Dosimetry
- Radiation Therapies
- Radiation Shielding
- Materials Damage



The Influence of Stopping Powers upon Dosimetry for Radiation Therapy with Energetic Ions

Helmut Paul¹, Oksana Geithner² and Oliver Jäkel²

¹Institut für Experimentalphysik, Atom- und Oberflächenphysik, Johannes-Keppler-Universität, Altenbergerstraße 69, A-4040 Linz, Austria

²Department of Medical Physics, German Cancer Research Center (DKFZ), D-69120 Heidelberg, Germany

Abstract

Following a recent recommendation from the International Atomic Energy Agency (IAEA), air filled ionization chambers (calibrated in terms of absorbed dose to water) should be used for the dosimetry in radiation therapy with fast ions. According to IAEA, the main source of uncertainty in the dose determination is resulting from the stopping power ratio water to air, which is introduced in order to convert the dose measured in the air cavity to the dose to water, which is used as the standard reference medium. We show that our knowledge of suitable stopping power data is very limited, but that the dependence of the stopping power ratio on the mean ionization energies I_{water} and I_{air} is dominating this quantity over a large energy range. We discuss the I -values used in ICRU Reports 37, 49, and 73, and we show how the various choices affect the ratio of stopping powers and the stopping power ratio. In doing so, we also investigate a choice of I -values differing from the ICRU recommendations. The stopping power ratio is defined as the fluence-weighted average ratio of stopping powers using the Monte Carlo program SHIELD-HIT 4.2 for carbon, carbon ions at 50 and 400 MeV/nucleon, including the effect of secondary fragments produced by nuclear reactions.

Using a single set of I -values for all primary and secondary particles, we find that the stopping power ratio hardly differs from the simple ratio of stopping powers for C ions over a large energy range. Compared to an earlier result [O. Geithner et al., *Phys. Med. Biol.* 51 (2006) 2279] there are some minor differences, arising from a combination of different I -values from different stopping power tables (ICRU 49 for protons and alphas, ICRU 73 for the heavier ions).

For the very low energy region, which is important for dosimetric measurements close to the Bragg peak, the simple ratio of stopping powers is no longer valid. When using a consistent set of I -values it is shown that the deviation of the stopping power ratio (including nuclear fragmentation) from the recommendation of IAEA is very small at high energies, but increases up to 3% in the stopping region.

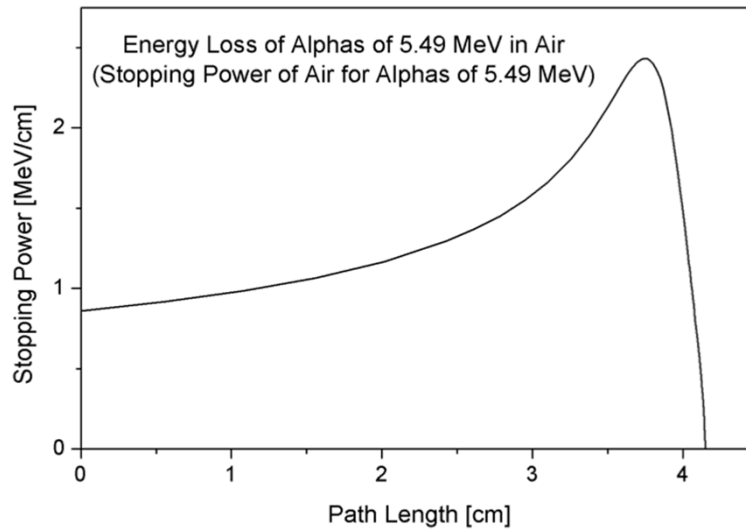
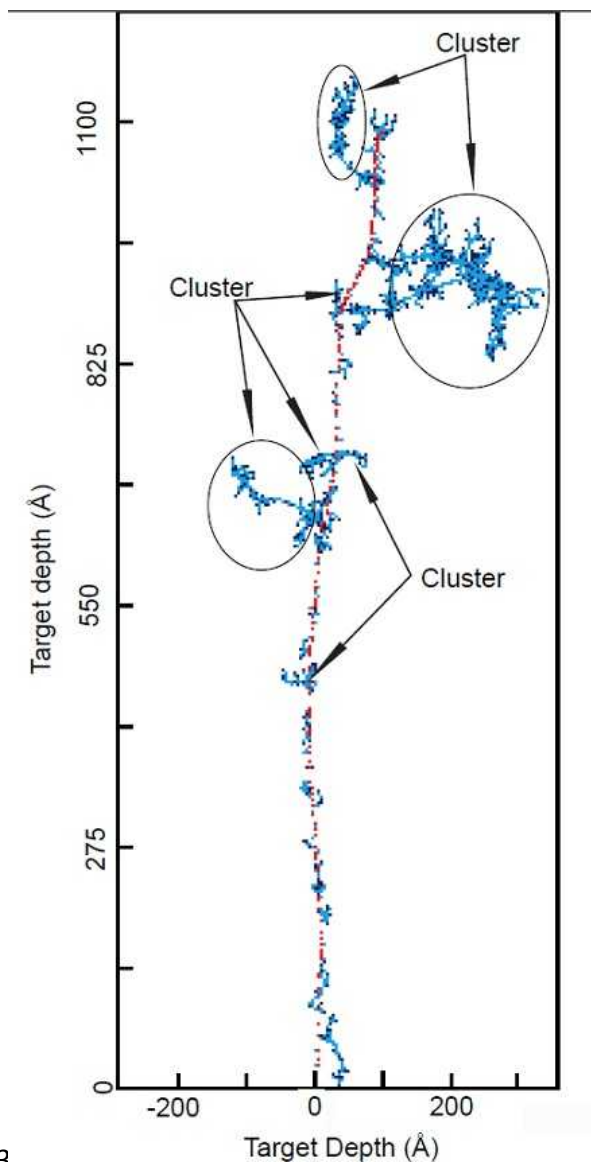
Concerning future investigations, we think it is worthwhile to reanalyze the various sources of I -values taking into account not only stopping power data but also precision range measurements, since the calculated ranges critically depend on the selected I -value.

Contents

1. Introduction	290
2. Stopping power	291
2.1. Definition	291
2.2. Experimental data, available tables and computer codes	292
3. I values for water and air	294
3.1. I values for air	295
3.2. I values for water	297
4. Stopping power ratios for dosimetry	299
4.1. Ratios of stopping powers	299
4.2. Stopping power ratios	301

© 2007 Elsevier Inc.
All rights reserved

Stopping Power



$$S(E) = -\frac{d}{dx} E_{\text{Proj.}}$$

Penetration Depth :

$$\Delta x = \int_0^{E_0} dE \frac{1}{S(E)}$$

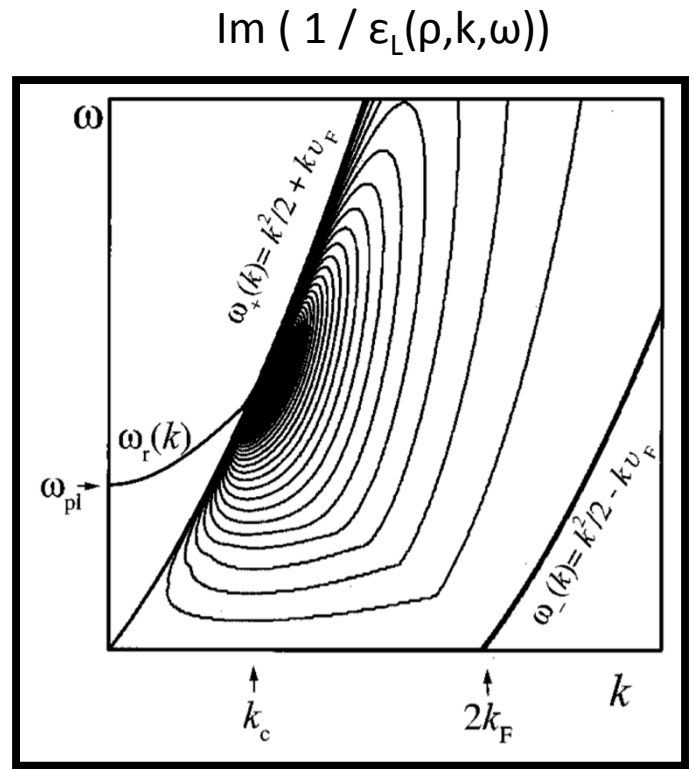
Common Materials Monte Carlo Data Tabulated:
www.srim.org

Lindhard Stopping

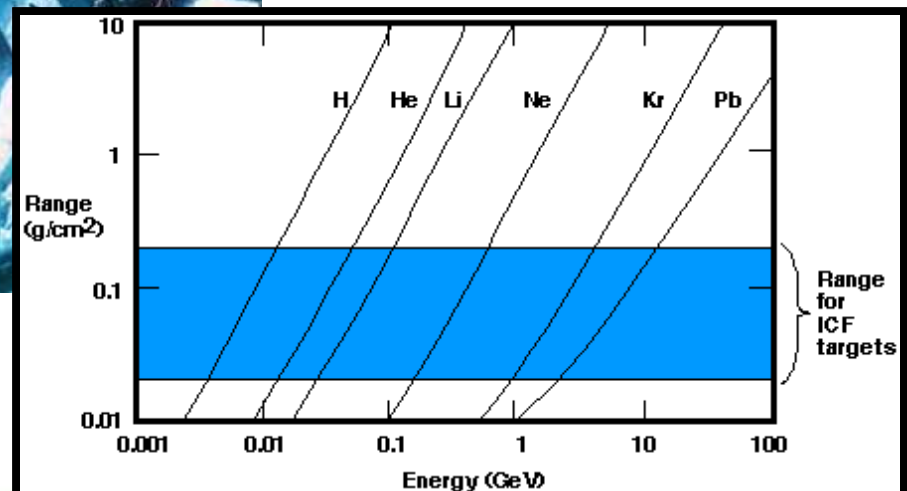
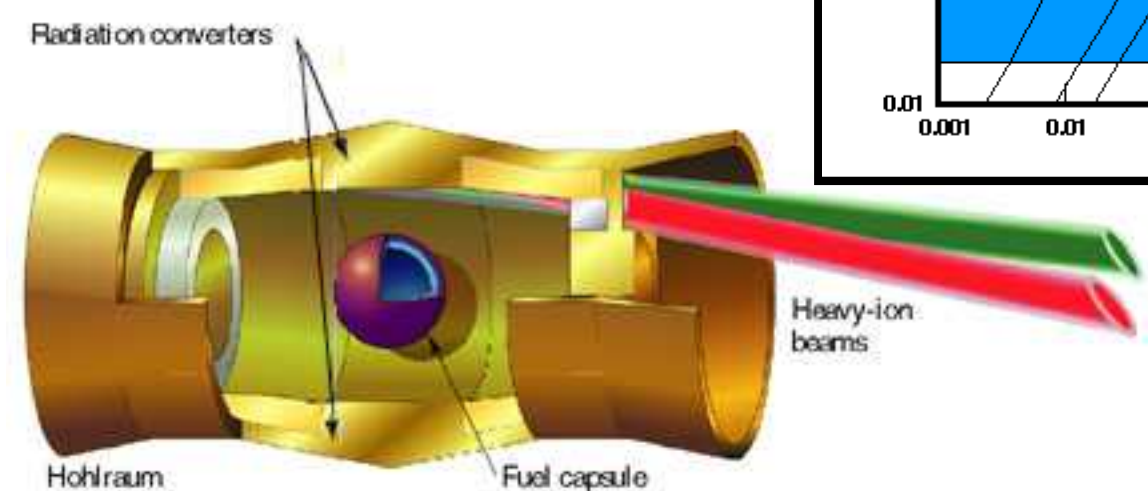
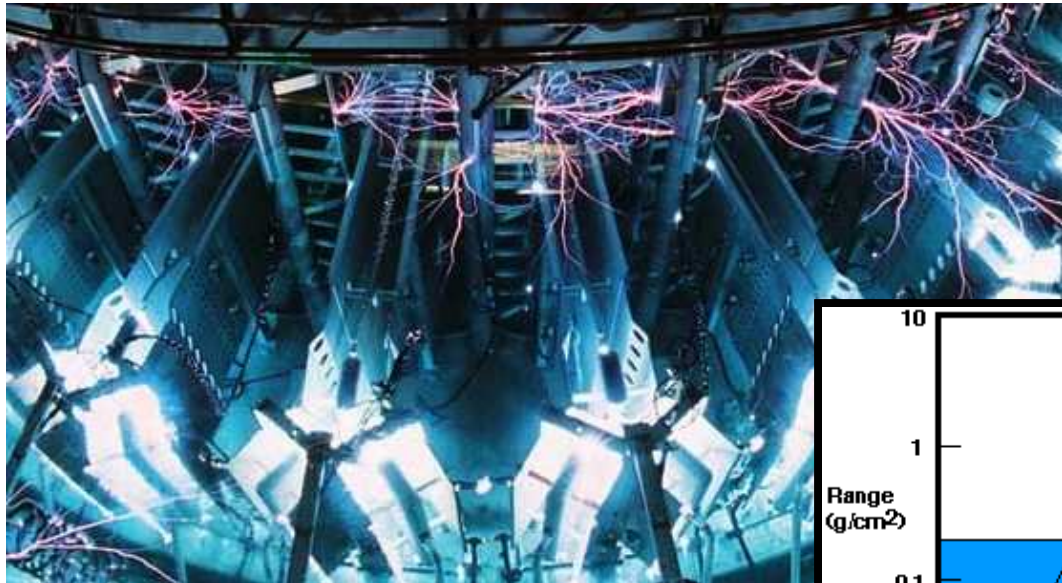
$$-\frac{dE}{dx} = \frac{4\pi}{m} \left(\frac{Ze^2}{v} \right)^2 \rho L(\rho, v)$$

$$L(\rho, v) = \int_0^{\infty} \frac{dk}{k} \int_0^{\omega_p} d\omega \omega \operatorname{Im} \left[\varepsilon(\rho, k, \omega)^{-1} \right]$$

- Relate stopping power to dielectric response function
- Find dielectric response in perturbation theory

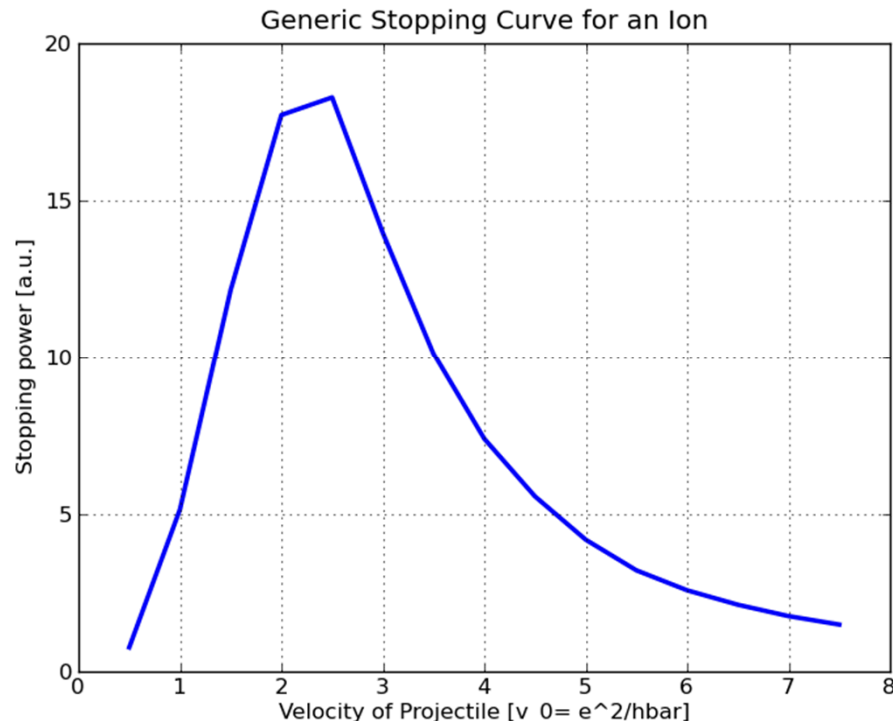


Inertial Confinement Fusion and Warm Dense Matter



Energy Regimes in Stopping Power

- Low energy $v < 0.1$ a.u. ground-state or thermal electrons / adiabatic regime
- High energy $v >> 0.1$ a.u. electron dynamics
- Intermediate regime: combined electron-nuclear dynamics, electron capture and ionization



Approaches to Stopping in Real-Time Electron Dynamics Simulations

1. Total energy – Constant velocity projectile, increasing total energy of system
2. Forces on nuclei – Direct solution of forces of projectile
3. Perturbative – Relationship to dielectric response of system

J.M. Pruneda et al. Nuclear Instruments and Methods in Physics Research B 267 (2009) 590–593

J. M. Pruneda, D. Sánchez-Portal, A. Arnau, J. I. Juaristi, and E. Artacho, Electronic stopping power in LiF from first principles, Phys. Rev. Lett. **99**, 235501 (2007).

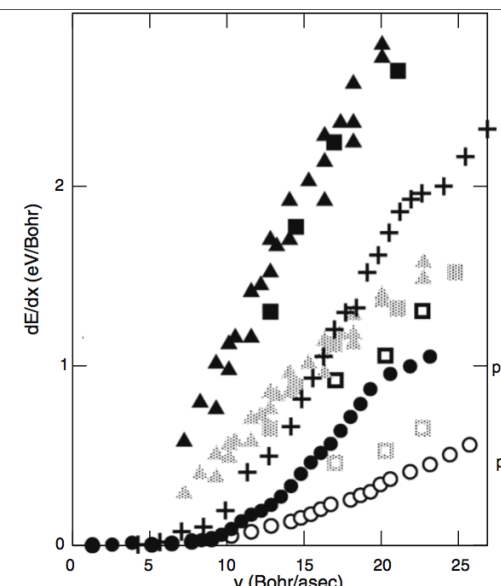
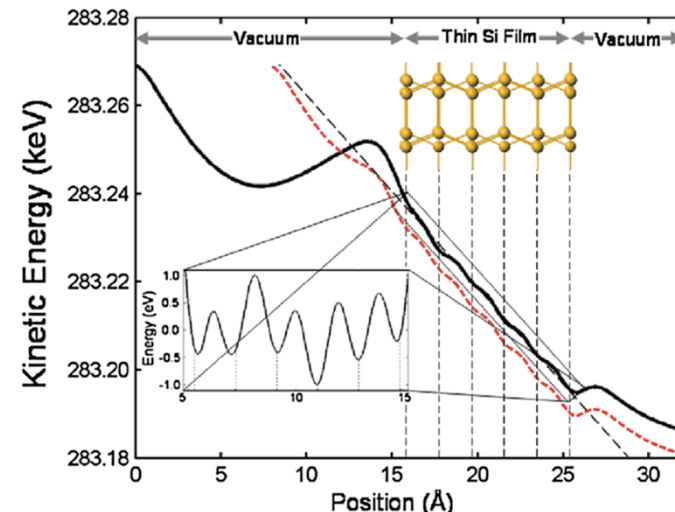


Fig. 1. Electronic stopping power $\frac{dE}{dx}$ as a function of the particle velocity v for p (filled symbols) and p (empty symbols). Circles are the calculations while triangles and squares indicate, respectively, the measured values of [9] and [10]. Grey triangles and squares are these measured values scaled by 1/2, for direct comparison with the calculations, which only considered channelling trajectories. Crosses indicate calculations for p including additional basis orbitals along the projectile's path (see text).



R. Hatcher, M. Beck, A. Tackett, and S.T. Pantelides, Phys. Rev. Lett. 100, 103201 (2008).

Electron-Dynamics through TDDFT

Time-dependent KS Scheme Builds Upon the Highly Successful Ground-state Theory

$$i \frac{\partial}{\partial t} \phi_i(r, t) = \left[-\frac{1}{2} \nabla^2 + v_{KS}[\Psi_0, \Phi_0, n](r, t) \right] \phi_i(r, t)$$

$$\phi_i(r, 0) = \phi_i^T(r) \quad \int d^3r \phi_i(r, t) \phi_j(r, t) = \delta_{ij}$$

$$n(r, t) = \sum_i^{occ.} |\phi_i(r, t)|^2$$

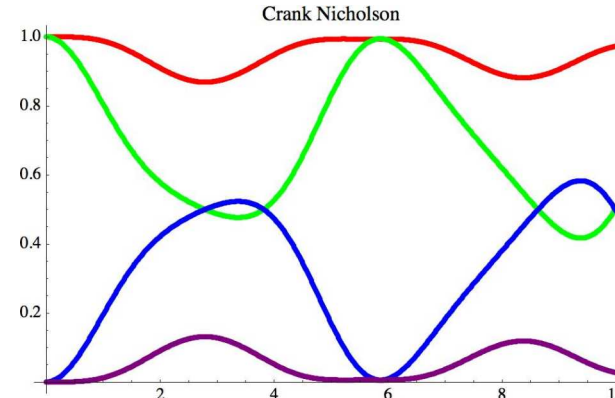
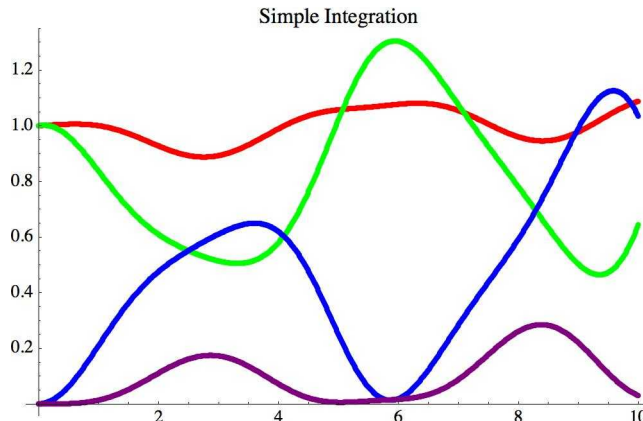
In the spirit of KS DFT, we postulate that a non-interacting system with a judiciously chosen potential can reproduce the time dependent density.

$t_{\text{electron}} \ll t_{\text{nuclei}}$ for long simulations 50000 time steps typical > 5000 in DFT-MD

Time Integration and Functionals Used

- Adiabatic approximate functionals (ALDA) is used
- Time-evolving external potential is applied for projectile
- Fixed bulk nuclei
- Various impact factors chosen to allow traversal of supercell
- Time-Propagation Schemes
 1. Naïve application of Runga-Kutta theory loses charge
 2. Split Matrix Operators
 3. Crank-Nicholson Unitary and Time-reversible
 4. Predictor corrector on a non-linear differential equation
 5. Velocity Verlet for nuclei

$$e^{-i\hat{H}\Delta t} \approx \frac{1 - i\hat{H}\Delta t/2}{1 + i\hat{H}\Delta t/2}$$



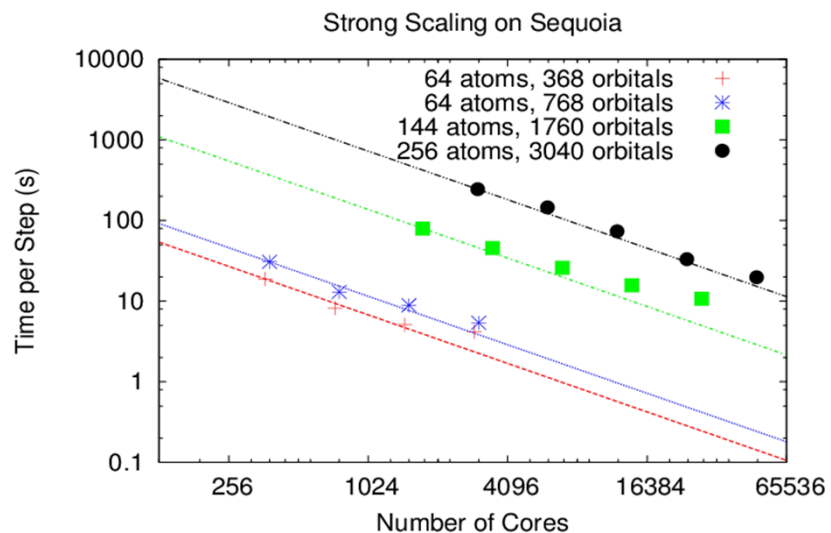
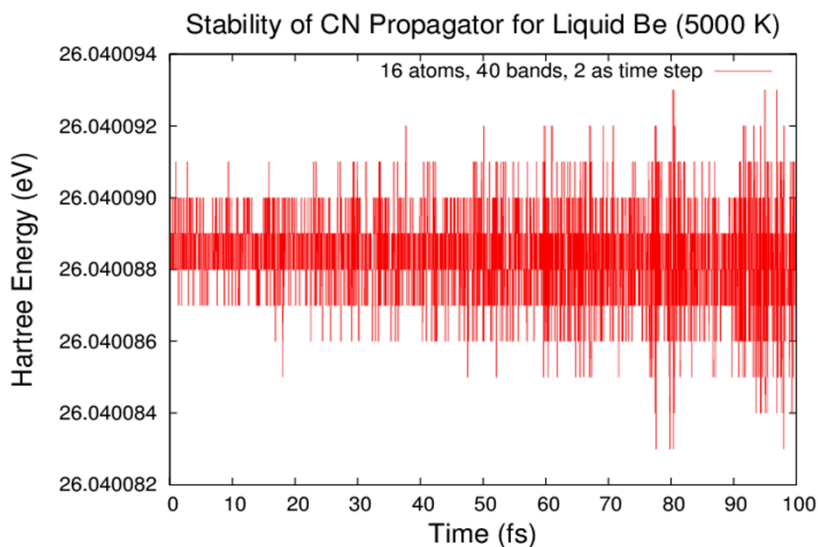
Projector-Augmented Plane-Wave (PAW) Calculations

$$\Psi = \hat{T} \tilde{\Psi} = \left[1 + \sum_{a,i} \left(|\phi_i^a\rangle - |\tilde{\phi}_i^a\rangle \right) \langle \tilde{p}_i^a | \right] \tilde{\Psi}$$

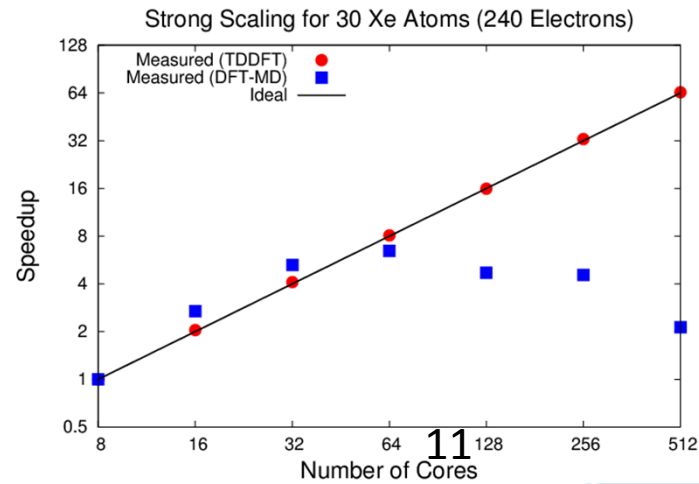
$$i\hat{S} \frac{\partial}{\partial t} \tilde{\Psi} = (\hat{H} + \hat{P}) \tilde{\Psi}$$

$$\hat{S} = \hat{T}^\dagger \hat{T} \quad \hat{P} = -i \hat{T}^\dagger \frac{\partial}{\partial t} \hat{T}$$

Stable and Scalable Implementation of TDDFT



Capability calculations in Sequoia!
Stable over many time steps often >50000



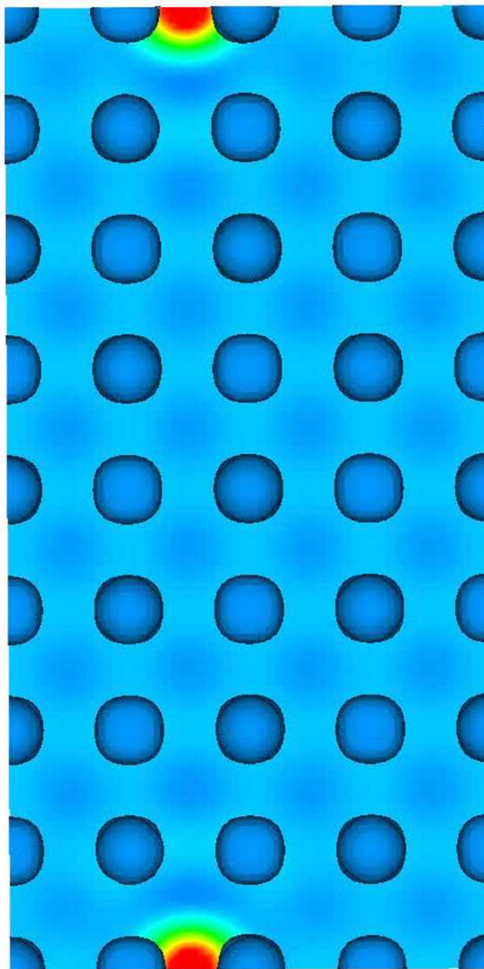
Coupled Electrons and Moving Nuclei

$$H[\{R_I\}]\phi = \varepsilon\phi \quad \text{vs.} \quad H[\{R_I\}]\phi = i\frac{d}{dt}\phi$$
$$F_I = -\left\langle \nabla_I V(\{R_I\}) \right\rangle$$

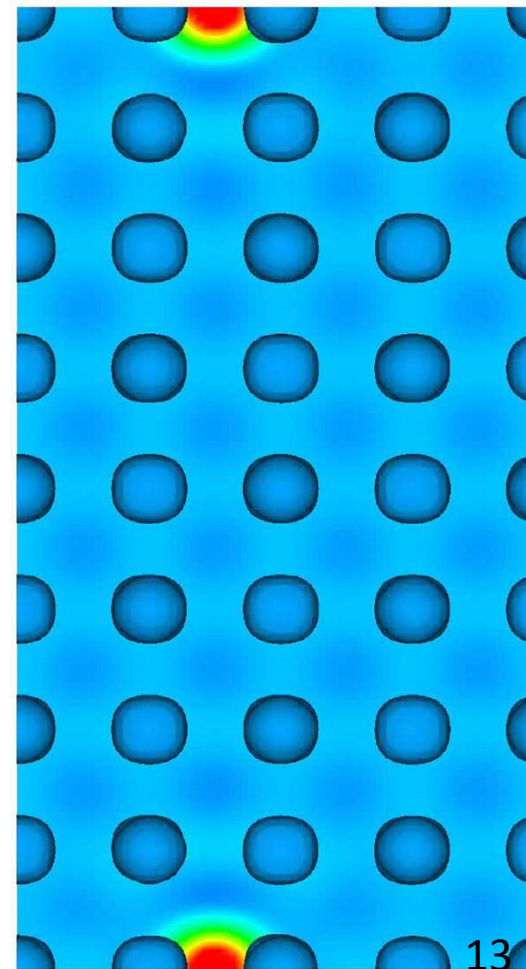
- **Separate model for coupled electron ion dynamics**
- No uncoupled electron dynamics Born-Oppenheimer
- Electron-dynamics in Ehrenfest
- Certain processes not described by even Ehrenfest such as photochemistry, discrete electron relaxation

Born-Oppenheimer vs. Ehrenfest

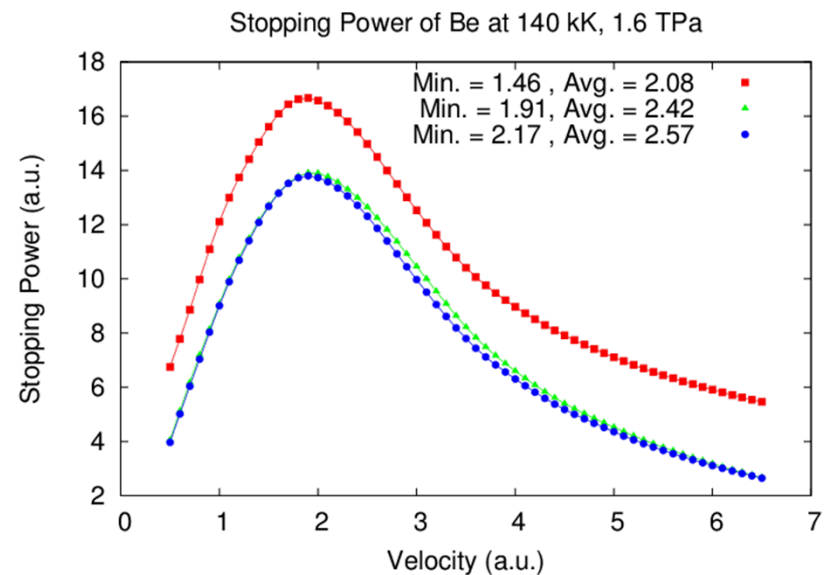
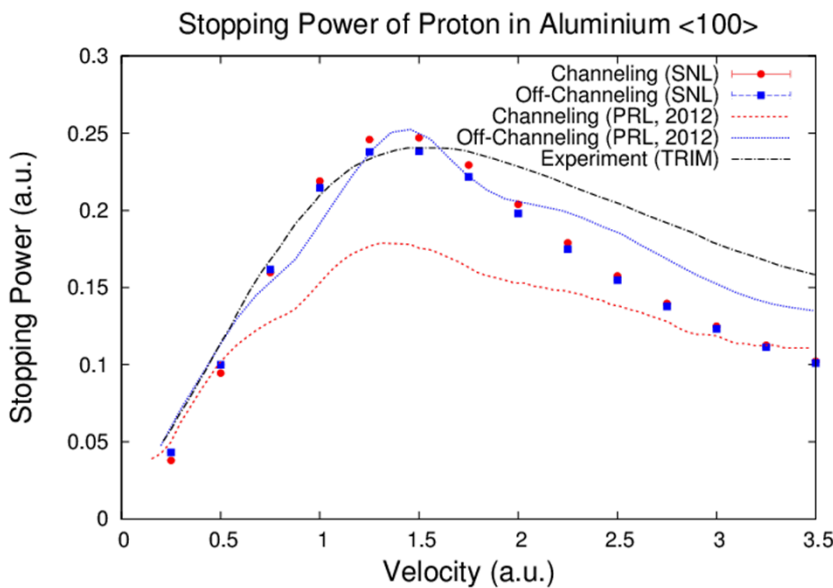
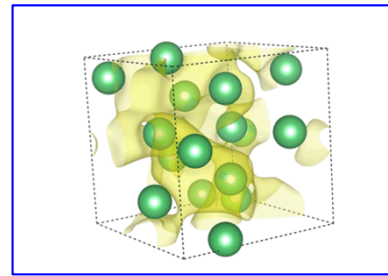
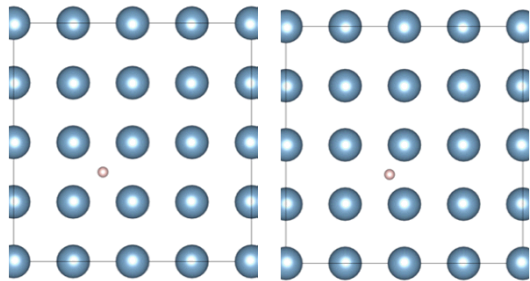
Born-Oppenheimer



Ehrenfest



Stopping Power Calculations Extended to WDM



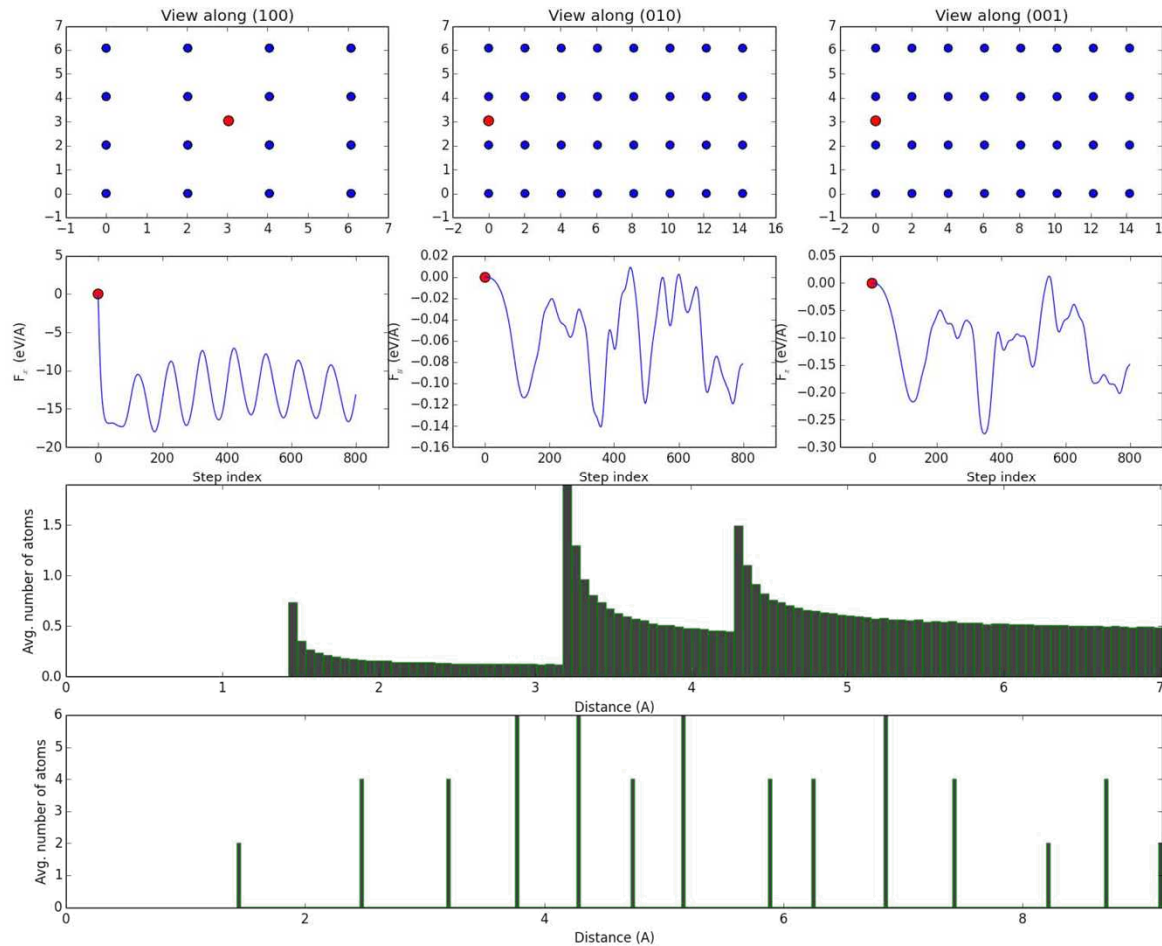
Accurate atomistic first-principles calculations of electronic stopping
André Schleife, Yosuke Kanai, and Alfredo A. Correa
Phys. Rev. B 91, 014306 – Published 20 January 2015

Coupling Electron-Nuclear Motion

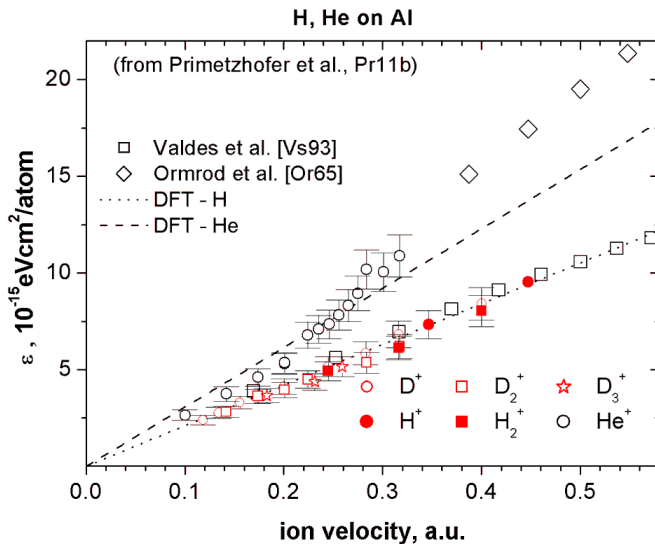
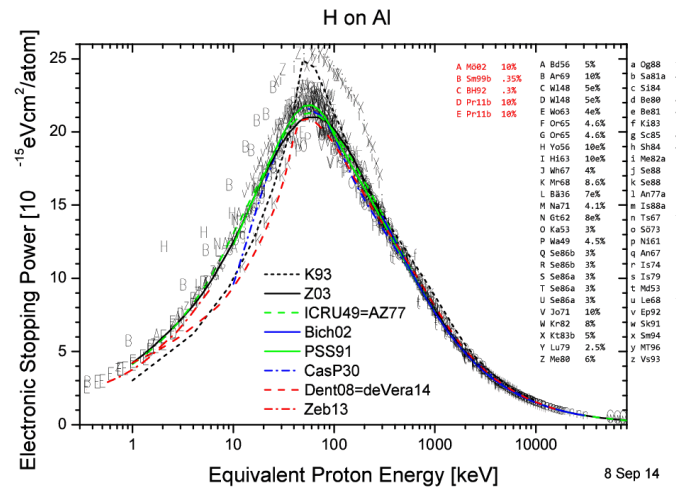
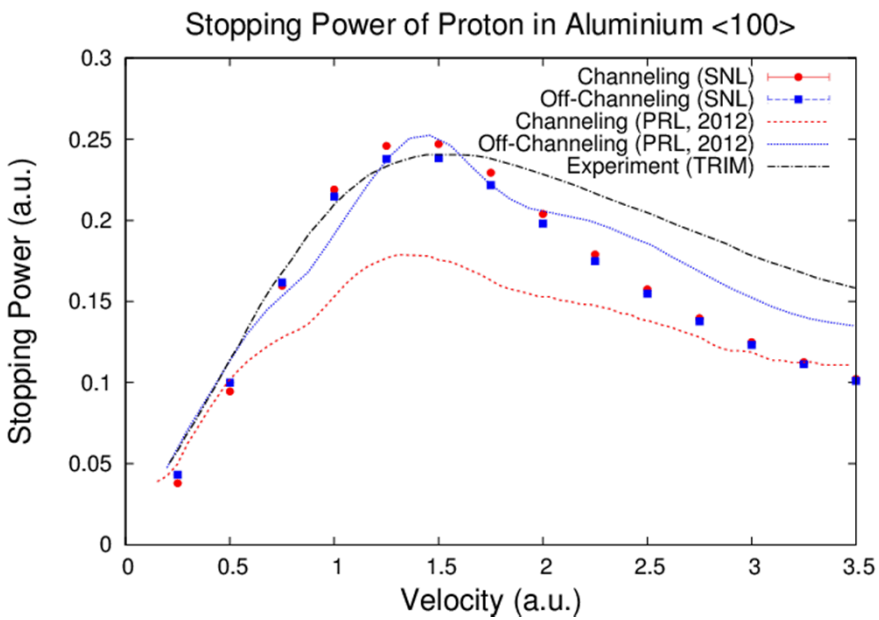
1. Conservation of Instantaneous Total Energy – “Adiabatic Approximation”
2. Energy conservation plus Pulay forces
3. Stationary action derived forces

Choice affects both electrons and nuclei at each time step!

Calculations of Stopping



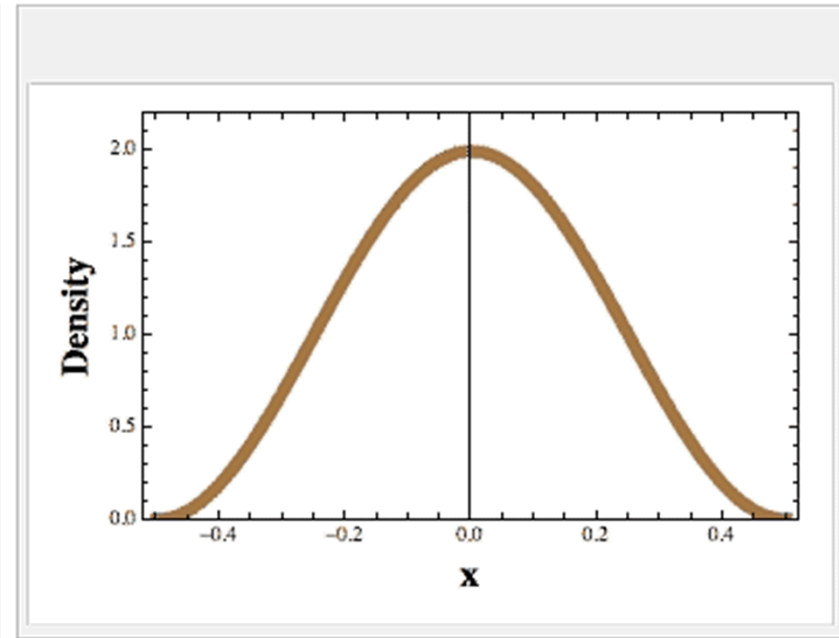
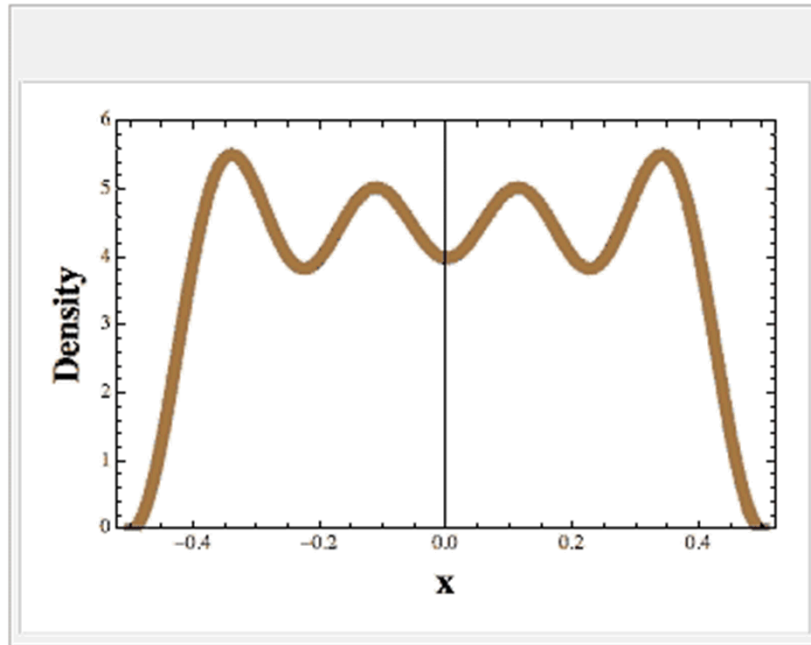
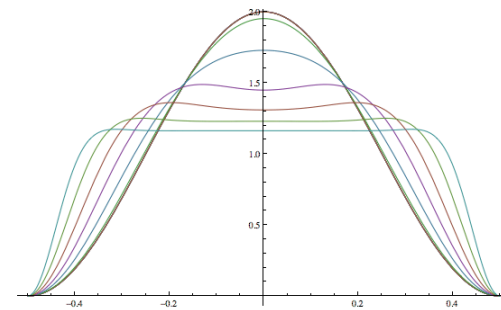
TDDFT on Aluminum vs. Literature



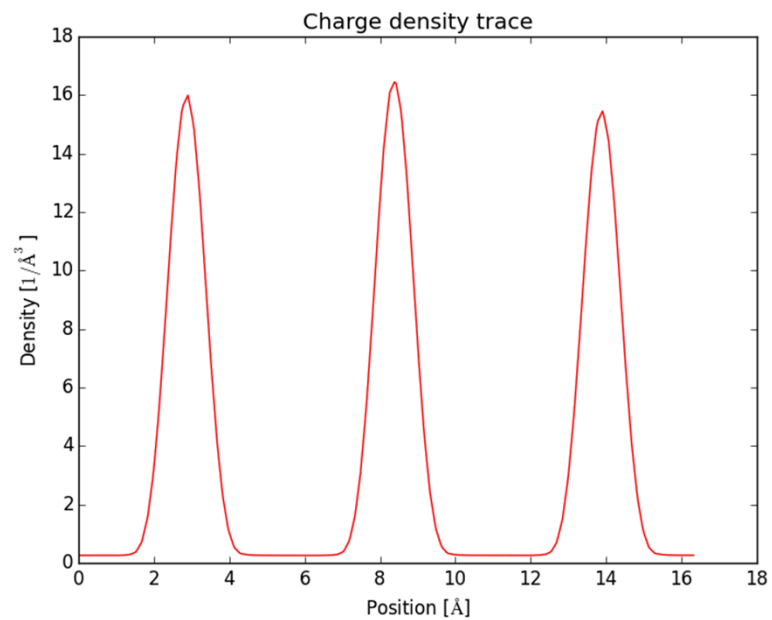
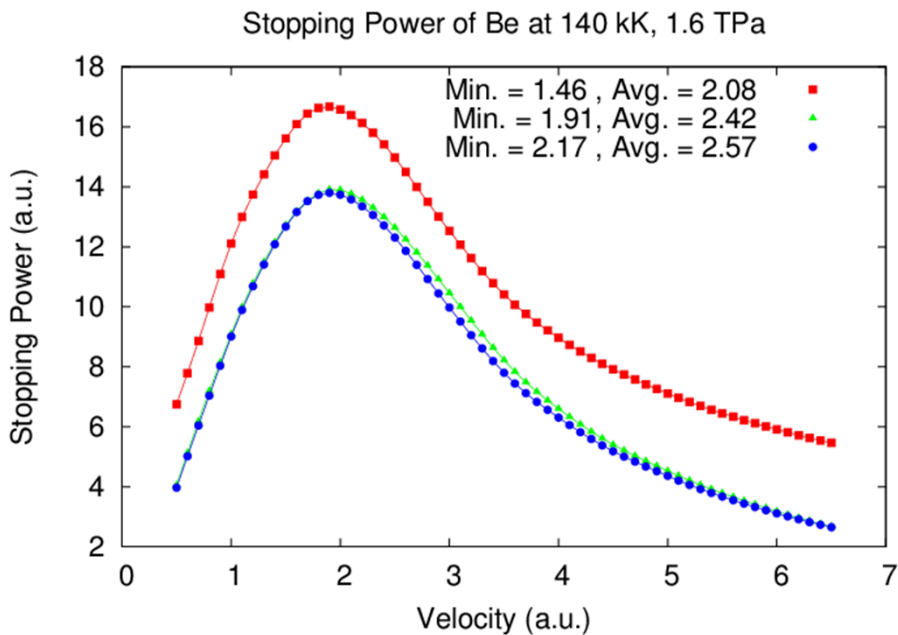
TDDFT on WDM

Mermin DFT propagated in time

$$n(r, t) = \sum_i^{\text{occ.}} f_i |\phi_i(r, t)|^2, f_i \leq 1$$

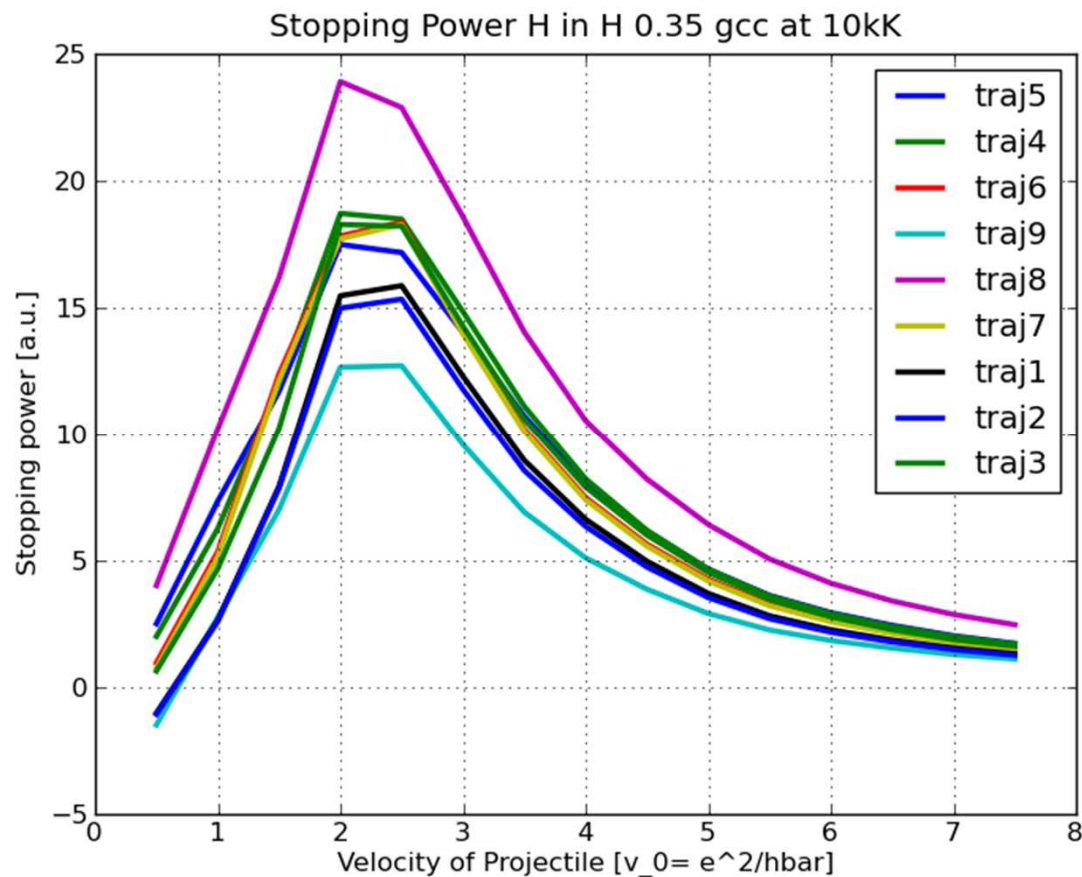


Stopping Power in Be



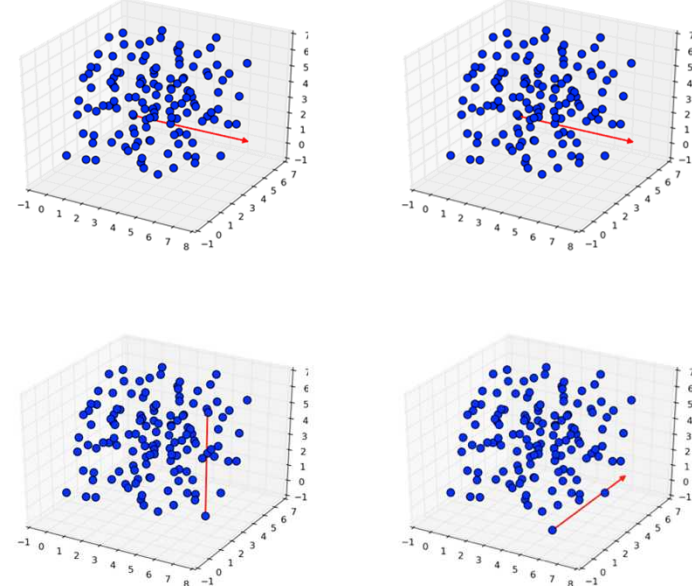
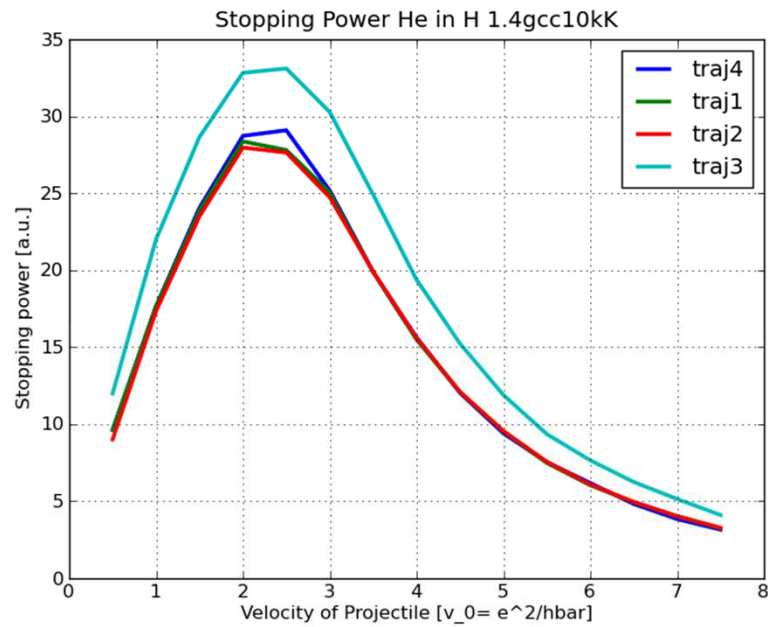
H in H at 1000 K

- Liquid density at ambient 0.07 gcc



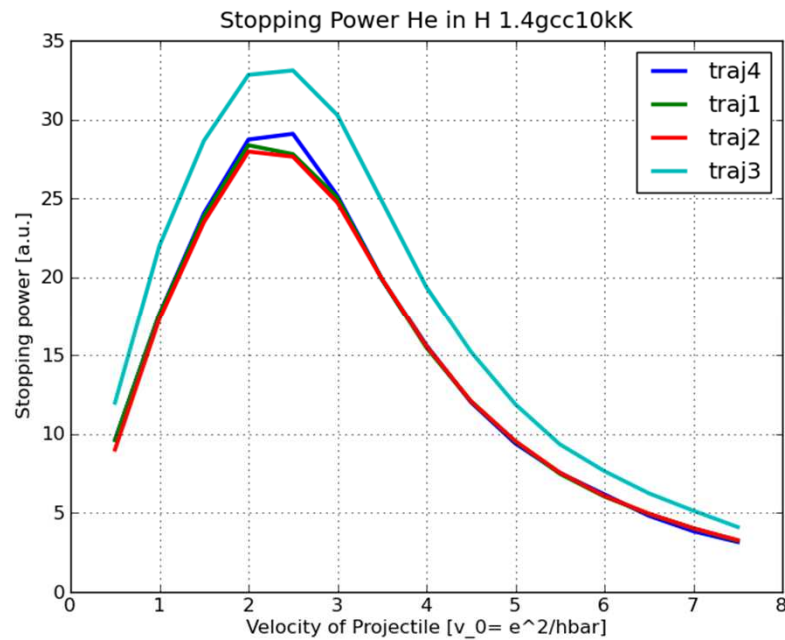
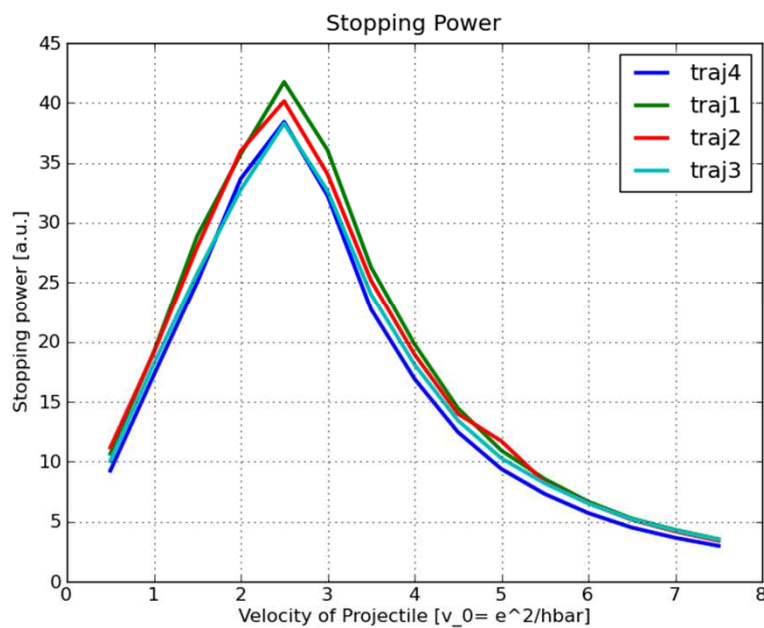
Results for Warm He in D stopping

1.4 gcc at 10,000 K

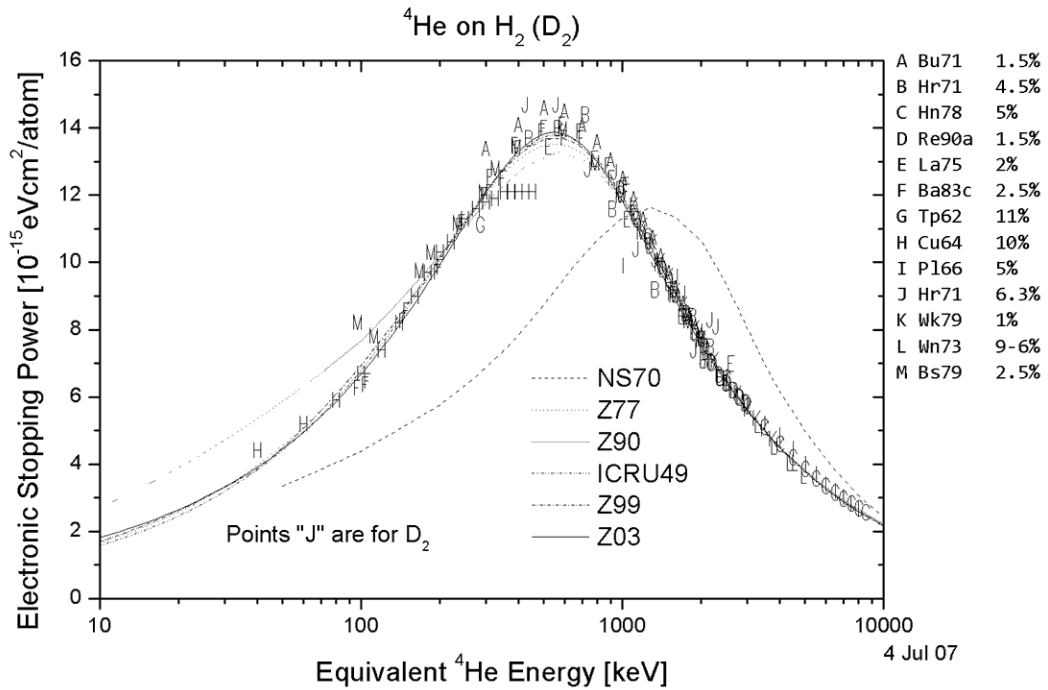
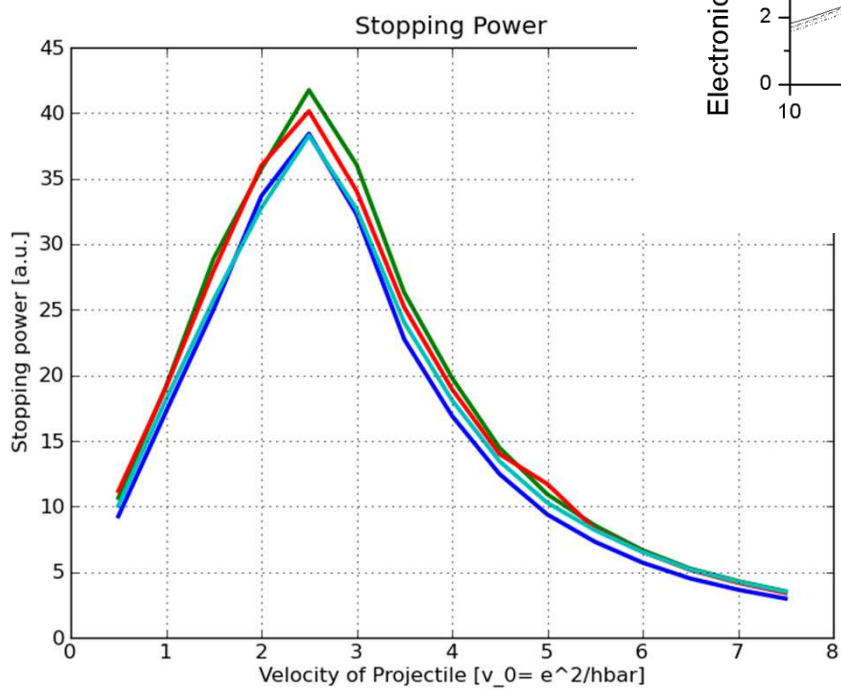


Incomplete forces needed for stability
but charge is no longer fully conserved

Stopping Vs. Temperature 1000K and 10000K D at 1.4 gcc



Warm He in D



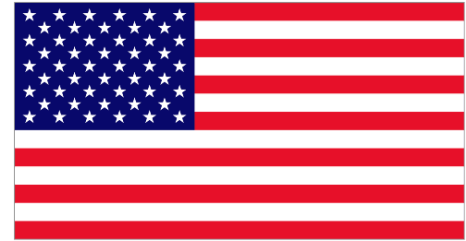
Conclusions

TDDFT allows us to calculate stopping powers in regimes that are hard to probe experimentally

Challenges remain regarding the best time integration schemes that conserve charge and provide accurate and stable simulations.

Acknowledgments

- LDRD
- Science campaign funding
- Sandia High-Performing Computing (HPC)
- Sequoia CCC6, CCC7



Some considerations

- **Translational invariance**

$$\Psi_n(x, t) = \exp(-i\varepsilon_n t + i\omega x) \Psi_n(x + \omega t, t)$$

Electron-Ion Equilibration

Hot ions and cold electrons or Hot electrons and cold ions

Often modeled in terms of a 2 temperature model

$$T_{\text{Equilibration}} = 0.33 - 10 \text{ ps}$$

Runge-Gross Leaves the Question of Weights Open

- Different representations of TDDFT ensemble densities
- NVT thermal density but NVE propagation?!

$$\hat{\rho}^{\text{Exact}} = \sum_i W_{i,\beta} |\Psi_i\rangle\langle\Psi_i|$$

$$\hat{\rho}^{\text{Mermin}} = \sum_i w_{i,\beta} |\phi_i(w_{i,\beta})\rangle\langle\phi_i(w_{i,\beta})|$$

